

# BATCHED TRAINING FOR QLSTM VS. QFWP: A SYSTEM-ORIENTED APPROACH TO EPC-AWARE RMSE-DA

Jun-Hao Chen<sup>1</sup>, Ming-Kai Hung<sup>1</sup>, Yun-Cheng Tsai<sup>1</sup>, Samuel Yen-Chi Chen<sup>2</sup>

<sup>1</sup>Department of Technology Application and Human Resource Development,  
National Taiwan Normal University, Taipei, Taiwan

<sup>2</sup>Wells Fargo Bank, USA

## ABSTRACT

We compare two quantum sequence models, QLSTM and QFWP, under an Equal-Parameter-Count (EPC; trainable-parameter) and adjoint-differentiation setup on daily EUR/USD forecasting as a controlled 1D time-series case study. Across 10 random seeds and batch sizes 4–64, we measure component-wise runtimes (train-forward, backward, full-train, and inference) and accuracy (RMSE and Directional Accuracy (DA)). Batched forward scales well ( $\sim 2.2\text{--}2.4\times$ ), but backward scales modestly (QLSTM  $\sim 1.01\text{--}1.05\times$ , QFWP  $\sim 1.18\text{--}1.22\times$ ), capping end-to-end training speedups near  $2\times$ . QFWP attains lower RMSE and higher DA at all batches (Wilcoxon  $p \leq 0.004$ , large Cliff's  $\delta$ ), while QLSTM reaches the highest throughput at batch 64, revealing a clear speed-accuracy Pareto frontier. We provide an EPC-aligned, numerically checked benchmarking pipeline and practical guidance on batch choices; broader datasets and hardware/noise settings are left for future work.

**Index Terms**— quantum machine learning, batching, QLSTM, QFWP, performance analysis

## 1. INTRODUCTION

Quantum sequence models have gained traction for signal processing tasks that require learning long-range dependencies [1, 2, 3]. Among these, QLSTM augments classical memory with variational quantum circuits [4], while programmable architectures such as QFWP avoid recurrent quantum states by using a slow classical network to configure shallow circuits at each step [5, 6]. Despite this progress, systematic benchmarking under batching and adjoint differentiation remains limited. Prior work emphasizes architectural efficiency [7, 8], yet few studies quantify forward and backward scaling or accuracy stability across batch sizes [9].

This paper closes these gaps by presenting a unified Equal-Parameter-Count (EPC) benchmark of QLSTM and QFWP on a canonical OHLC→next-day-close forecasting task, with EUR/USD as a representative 1D case study for controlled system measurement. We define EPC over *trainable* parameters, report the quantum/classical split, and de-

compose wall-clock time into train-forward, backward, full-train, and inference components to expose adjoint-gradient bottlenecks. Forward pass speedups scale strongly with batching, while backward pass scaling remains modest, yielding end-to-end gains of  $\sim 2\times$ . Under this fixed-epoch training budget, QFWP achieves lower RMSE and higher DA, whereas QLSTM provides the highest throughput, forming a clear speed-accuracy Pareto frontier.

## 2. METHODOLOGY

**Task and Data.** We use daily EUR/USD OHLC (Dec 2003–Dec 2024, seq-len 5) with an 80/20 train–test split. Each rolling window is min–max normalized; the same scale is applied to the target. We report RMSE and Directional Accuracy (DA) on the original scale:

$$\text{DA} = \frac{100}{|\mathcal{I}|} \sum_{t \in \mathcal{I}} \mathbf{1}[\text{sign}(\hat{y}_t - \hat{y}_{t-1}) = \text{sign}(y_t - y_{t-1})],$$

where  $\mathcal{I} = \{t : y_t \neq y_{t-1}\}$ . We use a single 1D dataset to isolate system effects.

**Quantum Models.** QLSTM [4] replaces each LSTM [10] gate with a shallow VQC [11] operating on  $[\mathbf{x}_t; \mathbf{h}_{t-1}]$ , where  $\mathbf{x}_t \in \mathbb{R}^4$  and  $\mathbf{h}_{t-1} \in \mathbb{R}^H$ . Each gate outputs  $\mathbf{e}_t^{(g)} = \text{VQC}_g([\mathbf{x}_t; \mathbf{h}_{t-1}]; \Theta_g)$  and uses  $\sigma/\tanh$  to update  $\mathbf{c}_t = \mathbf{f}_t \odot \mathbf{c}_{t-1} + \mathbf{i}_t \odot \tilde{\mathbf{c}}_t$  and  $\mathbf{h}_t = \mathbf{o}_t \odot \tanh(\mathbf{c}_t)$ , with  $y_t = W_{\text{out}} \mathbf{h}_t + b_{\text{out}}$ . Each VQC (depth 1) initializes  $n_q = 4 + H$  wires in  $|+\rangle$ , encodes via  $R_y$ , applies an even–odd CNOT ladder, and measures  $\mathbb{E}[Z]$  on the first  $H$  wires. With  $H = 3$ , QLSTM has 32 trainable parameters (28 quantum + 4 classical).

QFWP [5] follows fast-weights [12, 13]: a slow classical network *programs* a shallow circuit each step. Given  $\mathbf{s}_t$  (OHLC), it computes  $\mathbf{z}_t = W_e \mathbf{s}_t + b_e$ , selectors  $\boldsymbol{\alpha}_t = W_\ell \mathbf{z}_t + b_\ell$  and  $\boldsymbol{\beta}_t = W_q \mathbf{z}_t + b_q$ , and updates angles  $\Theta_t = \Theta_{t-1} + \boldsymbol{\alpha}_t \boldsymbol{\beta}_t^\top$  ( $D = 1$ ,  $Q = 3$ ). The VQC encodes  $\mathbf{s}_t$  with  $R_y$ , applies one entangling layer, measures  $A = 1$ , and predicts  $\hat{y}_t = W_p \mathbf{a}_t + b_p$ . All 33 trainable parameters are classical; per-step angles are generated by the slow net (see Table 1). Both models are EPC-aligned and implemented in

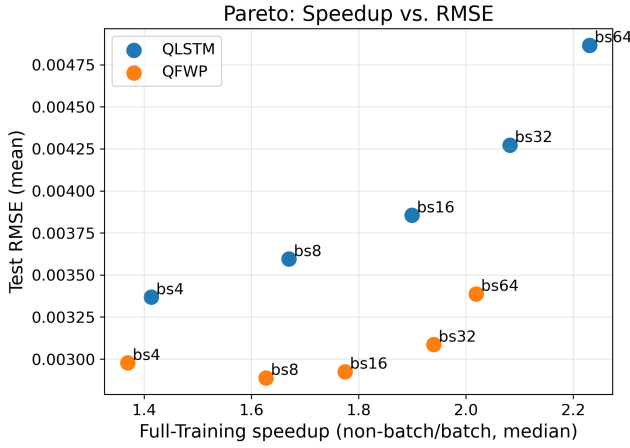


**Fig. 1.** Pareto view: full-training speedup (median) vs. RMSE (mean). Each point is annotated with its batch size, and marker styles distinguish QLSTM vs. QFWP for grayscale readability.

PennyLane [14] (`lightning.qubit`) with PyTorch [15] autograd (`diff_method=adjoint`).

**Training and Evaluation Protocol.** We compare non-batch vs batch sizes  $\{4, 8, 16, 32, 64\}$  over 10 seeds using identical splits and synchronized initialization. For each run we time: (1) Train-Forward, (2) Backward, (3) Full-Training (2 epochs, fixed budget), and (4) Inference-Forward (after warm-up). Speedup is  $T_{\text{non-batch}}/T_{\text{batch}}$  summarized as median [IQR]; accuracy is  $\text{mean} \pm \text{std}$ . We fix epochs (not steps) to emphasize throughput, yielding fewer updates at larger batches (4,374 samples  $\rightarrow$  1,094/547/274/137/69 steps per epoch for batch 4/8/16/32/64). No gradient accumulation or LR scaling is used.

**Numerical Checks and Statistics.** We feed identical tensors to batched/non-batched implementations. For QLSTM we verify forward equivalence ( $L_2 \leq 10^{-6}$ ) and measure backward wall-time; for QFWP we verify forward equivalence only (per-sample adjoint cost). Across seeds, paired Wilcoxon signed-rank tests [16] compare QLSTM vs QFWP per batch, with Cliff’s  $\delta$  [17] effect sizes; timing medians [IQR] reveal scaling bottlenecks.

All experiments use a state-vector simulator (no hardware execution or noise modeling); timings therefore reflect relative simulation efficiency.

### 3. EXPERIMENTS AND RESULTS

#### 3.1. Main Accuracy Trends

Table 2 summarizes accuracy across seeds ( $\text{mean} \pm \text{std}$ ). Across all batches (4–64), QFWP consistently outperforms QLSTM in both RMSE and DA. Per batch Wilcoxon tests confirm significance for both metrics (all  $p \leq 0.004$ ),

with large effect sizes (for RMSE, Cliff’s  $\delta \geq 0.80$ ). QLSTM’s RMSE increases and DA decreases as batch grows, whereas QFWP remains stable through batch 16 and degrades more slowly thereafter. For example, as the batch size increases from 4 to 64, the mean RMSE for QLSTM rises from 0.00337  $\rightarrow$  0.00487, while QFWP increases from 0.00298  $\rightarrow$  0.00339. Over the same range, the mean DA drops from 69.04%  $\rightarrow$  58.67% for QLSTM and 72.72%  $\rightarrow$  65.84% for QFWP. Notably, QFWP maintains both lower error and higher directional skill at every batch, indicating that its advantage is not confined to a single operating point but persists under reduced update frequency. Variance also remains controlled for both models, although DA variance widens for QFWP at batch 64, suggesting that very large batches can increase sensitivity to initialization even when mean performance remains strong.

#### 3.2. Speed and Scaling

Tables 3 and 4 report per component times and speedups (median [IQR]) across batch sizes. Train forward speedups are strong for both models (about  $2.15$  to  $2.42 \times$  across batches). Backward speedup is modest, QLSTM  $1.01$  to  $1.05 \times$  and QFWP  $1.02$  to  $1.22 \times$ , and thus caps the end to end full training speedup at about  $2 \times$ . Concretely, the full training median speedup is  $2.08 \times$  (QLSTM) vs.  $1.94 \times$  (QFWP) at batch 32, and  $2.23 \times$  vs.  $2.02 \times$  at batch 64. We do not observe any backward slowdowns (below  $1 \times$ ); backward remains the dominant bottleneck. Inference forward speedups stay near  $2 \times$  for both models, which is practically relevant because it indicates that batching benefits are not limited to training and can translate to evaluation or deployment throughput when batched queries are available. The IQR summaries further show that timing variability across seeds is small compared to the median gaps, supporting the stability of the reported scaling trends.

#### 3.3. Pareto Tradeoff

Figure 1 shows full training speedup (median) against test RMSE (mean), with each point annotated by batch size and model distinct marker styles to improve readability in grayscale. The union of these labeled points traces a clear Pareto frontier: (1) QFWP contributes the accuracy optimal frontier points up to about  $2.0 \times$  speedup (batch 8 to 64); (2) QLSTM extends the throughput end (rightmost points at batch 32 and 64) with higher RMSE. Therefore, users can pick batch sizes from 8 to 16 for a balanced regime, achieving approximately  $1.6$  to  $1.9 \times$  speedup with minimal RMSE drift for QFWP. Alternatively, batch size 32 may be preferred when prioritizing speed (QLSTM) or error (QFWP). This frontier view emphasizes that batching is a tunable system parameter: increasing batch size moves along a predictable efficiency axis, while the two architectures occupy distinct

**Table 1.** Detailed parameter breakdown for EPC alignment.

Model	Total	Quantum	Classical	Architecture
<b>QLSTM</b> (input=4, hidden=3, $q_{\text{depth}} = 1$ , $n_{\text{qubits}} = 7$ )				
4 VQC gates	28	28	0	$4 \times (1 \times 7)$
output_post_processing	4	0	4	Linear(3→1)
<i>Subtotal</i>	32	28	4	—
<b>QFWP</b> ( $s_{\text{dim}} = 4$ , $a_{\text{dim}} = 1$ , latent=3, $n_{\text{qubits}} = 3$ , $q_{\text{depth}} = 1$ )				
slow_program_encoder	15	0	15	Linear(4→3)
slow_program_layer_idx	4	0	4	Linear(3→1)
slow_program_qubit_idx	12	0	12	Linear(3→3)
post_processing	2	0	2	Linear(1→1)
<i>Subtotal</i>	33	0	33	—
<b>Difference (QLSTM - QFWP)</b>	<b>-1</b>	—	—	<b>3.03%</b>

Note: QFWP’s quantum circuit parameters (3 per sample per step: 1 depth  $\times$  3 qubits) are not trainable; they are computed dynamically by the slow-programmer network.

**Table 2.** Accuracy across batch sizes ( $mean \pm std$  over seeds). Lower RMSE and higher DA are better. Per-batch significance uses Wilcoxon signed-rank test (QLSTM vs. QFWP); effect size reported as Cliff’s  $\delta$ .

Batch	RMSE (QLSTM)	RMSE (QFWP)	p-value	$\delta$ (RMSE)	DA (%) (QLSTM)	DA (%) (QFWP)
4	$0.0034 \pm 0.0001$	<b><math>0.0030 \pm 0.0002</math></b>	0.004	0.800	$69.04 \pm 0.89$	<b><math>72.72 \pm 1.88</math></b>
8	$0.0036 \pm 0.0001$	<b><math>0.0029 \pm 0.0001</math></b>	0.002	1.000	$67.89 \pm 0.64$	<b><math>72.75 \pm 0.93</math></b>
16	$0.0039 \pm 0.0001$	<b><math>0.0029 \pm 0.0001</math></b>	0.002	1.000	$65.56 \pm 0.75$	<b><math>72.34 \pm 0.79</math></b>
32	$0.0043 \pm 0.0002$	<b><math>0.0031 \pm 0.0002</math></b>	0.002	1.000	$62.34 \pm 1.22$	<b><math>70.18 \pm 2.74</math></b>
64	$0.0049 \pm 0.0003$	<b><math>0.0034 \pm 0.0004</math></b>	0.002	1.000	$58.67 \pm 0.95$	<b><math>65.84 \pm 4.29</math></b>

regions that favor either accuracy (QFWP) or maximum throughput (QLSTM).

#### 4. DISCUSSION

**Forward Backward Asymmetry and Its Systemic Implications.** Across all experiments we observe a pronounced asymmetry between forward and backward scaling under adjoint differentiation. With PennyLane state vector simulation and analytical reverse mode gradients, the forward path benefits strongly from batching because evaluating multiple samples in a single QNode call with parameter broadcasting reduces Python and QNode overhead and improves memory locality, resembling kernel fusion in classical deep learning. In contrast, the backward pass is dominated by the adjoint reverse time sweep that reconstructs and traverses the full computational graph. Its cost scales mainly with circuit depth, trainable parameter count, and unrolled sequence length, and only weakly with batch size. We therefore expect the asymmetry to increase for longer sequences or deeper circuits, and leave controlled sweeps over sequence length and quantum depth for future work. Empirically, forward speedup often exceeds  $2\times$  (about 2.2 to  $2.4\times$ ), whereas backward scaling saturates near  $1.0$  to  $1.22\times$  (QLSTM 1.01 to 1.05 $\times$ , QFWP 1.18 to 1.22 $\times$ ). The resulting end to end training speedup of about  $2\times$  matches an Amdahl style upper bound where the

backward fraction limits overall gain [18]. This indicates that gradient computation remains the main performance limiter. Potential remedies include alternative differentiators such as parameter shift with batched shifted circuits, or stochastic estimators on hardware, as well as update frequency control when large batches reduce step counts. QFWP shows slightly better backward scaling despite similar circuit depth, consistent with a smaller differentiation graph because its trainable parameters are classical and the quantum layer is driven by a compact slow programmer.

**Accuracy Dynamics and Optimization Robustness.** Batch size also changes accuracy through reduced update frequency under our fixed two epoch budget without gradient accumulation. QLSTM degrades rapidly as batch size increases from 4 to 64, with RMSE rising from 0.00337 to 0.00487 and DA dropping from 69.0% to 58.7%. QFWP remains stable through batch 16 ( $\text{RMSE} \approx 0.0029$ ,  $\text{DA} \approx 72.3\%$ ) and declines more slowly thereafter (batch 64  $\text{RMSE} \approx 0.0034$ ,  $\text{DA} \approx 65.8\%$ ). Across batches, paired Wilcoxon signed rank tests yield  $p \leq 0.004$  with large effect sizes (Cliff’s  $\delta \geq 0.80$ ), confirming a robust QFWP advantage. We attribute this to architectural decoupling: the slow programmer provides temporal coherence, and the outer product accumulation of fast parameters acts as an implicit stabilizer when updates are less frequent. More broadly, hybrid designs that delegate temporal structure to classical controllers appear more robust

**Table 3.** Batch implementation wall-clock time (seconds) per batch size: median [Q1, Q3] across seeds.

Model	Batch	Train-Forward	Backward	Full-Train	Infer-Forward
QLSTM	4	18.77 [17.71, 18.94]	1.36 [1.35, 1.38]	228.51 [226.83, 237.84]	15.80 [15.10, 16.65]
QLSTM	8	17.67 [16.79, 18.04]	1.35 [1.34, 1.38]	195.40 [194.03, 197.88]	15.38 [14.86, 16.36]
QLSTM	16	17.95 [16.36, 18.13]	1.33 [1.32, 1.38]	174.67 [174.10, 176.15]	16.18 [15.32, 16.57]
QLSTM	32	17.92 [16.49, 20.00]	1.36 [1.30, 1.38]	162.63 [160.49, 165.05]	16.09 [15.05, 16.41]
QLSTM	64	17.61 [16.84, 18.01]	1.35 [1.31, 1.36]	153.88 [152.64, 155.67]	15.92 [15.33, 16.46]
QFWP	4	2.66 [2.63, 2.78]	0.67 [0.67, 0.68]	42.23 [41.58, 43.20]	1.49 [1.47, 1.54]
QFWP	8	2.51 [2.48, 2.59]	0.79 [0.79, 0.80]	34.72 [34.41, 35.25]	1.56 [1.53, 1.58]
QFWP	16	2.54 [2.48, 2.58]	0.66 [0.66, 0.68]	31.53 [31.45, 31.63]	1.48 [1.46, 1.54]
QFWP	32	2.51 [2.48, 2.54]	0.66 [0.66, 0.67]	29.23 [28.77, 29.62]	1.67 [1.65, 1.69]
QFWP	64	2.63 [2.59, 2.67]	0.67 [0.66, 0.67]	27.95 [27.54, 28.50]	1.58 [1.53, 1.61]

Note: Train-Forward and Backward timings include Autograd graph construction, whereas Infer-Forward (model.eval() with torch.no\_grad()) does not. Full-Train is the total time over two epochs, including all mini-batches.

**Table 4.** Speedup (non-batch / batch) across batch sizes: median [Q1, Q3] over seeds.

Model	Batch	Train-Forward	Backward	Full-Train	Infer-Forward
QLSTM	4	2.15 [2.00, 2.20]	1.01 [0.98, 1.03]	1.41 [1.41, 1.43]	2.05 [1.88, 2.19]
QLSTM	8	2.20 [2.12, 2.31]	1.03 [0.98, 1.05]	1.67 [1.66, 1.69]	2.02 [1.94, 2.35]
QLSTM	16	2.29 [2.06, 2.45]	1.05 [1.01, 1.07]	1.90 [1.89, 1.92]	1.98 [1.89, 2.17]
QLSTM	32	2.20 [2.02, 2.36]	1.03 [1.01, 1.05]	2.08 [2.03, 2.13]	2.17 [1.95, 2.24]
QLSTM	64	2.42 [2.25, 2.57]	1.05 [1.03, 1.07]	2.23 [2.20, 2.48]	2.10 [2.07, 2.16]
QFWP	4	2.27 [2.11, 2.39]	1.19 [1.18, 1.20]	1.37 [1.34, 1.39]	2.32 [2.19, 2.39]
QFWP	8	2.30 [2.21, 2.40]	1.02 [1.02, 1.03]	1.63 [1.61, 1.64]	2.22 [2.18, 2.40]
QFWP	16	2.34 [2.22, 2.41]	1.20 [1.19, 1.22]	1.77 [1.74, 1.79]	2.29 [2.12, 2.39]
QFWP	32	2.35 [2.26, 2.39]	1.22 [1.19, 1.22]	1.94 [1.87, 2.00]	2.08 [2.01, 2.15]
QFWP	64	2.27 [2.23, 2.31]	1.20 [1.18, 1.21]	2.02 [1.95, 2.06]	2.18 [2.15, 2.26]

under throughput constrained training, while fully quantum gated recurrence is more sensitive to reduced backpropagated update counts.

## 5. CONCLUSION

This work presents a numerically grounded and EPC aligned comparison between QLSTM and QFWP under non batched and batched training, using adjoint differentiation on real EUR/USD forecasting data. Batching accelerates the forward pass but offers limited backward scaling, so full training speedup saturates near  $2\times$  by batch 32. Under a fixed two epoch budget, QFWP achieves lower RMSE and higher DA across all batch sizes (Wilcoxon  $p \leq 0.004$ , Cliff's  $\delta \geq 0.80$ ), while QLSTM attains the highest throughput at batch 64. Together, they form a speed accuracy Pareto frontier, with QFWP favoring accuracy and QLSTM favoring throughput. Beyond head to head results, this study provides a system level benchmark that isolates batch effects under adjoint differentiation and clarifies how quantum gated recurrence and hybrid controllers behave when throughput, precision, and gradient cost must be co optimized. The results suggest that scaling will depend on improved differentiators and training mechanics, not circuit design alone, and that EPC alignment is a practical diagnostic for deployable efficiency. Limitations include a single 1D financial dataset and simulator only backends. Future work will extend EPC benchmarking to other modalities and architectures.

**Pareto Frontier and Design Guidelines for Practitioners.** Figure 1 summarizes the trade off between accuracy and throughput. Over all batch sizes, QFWP occupies the accuracy optimal region ( $\text{RMSE} < 0.0032$ ,  $\text{DA} > 70\%$ ) for speedups below  $2\times$ , while QLSTM dominates the highest throughput region above  $2\times$  with higher error. This suggests complementary operating regimes rather than direct competition. For accuracy critical or inference sensitive workloads, QFWP with batch 8 to 16 offers the best balance ( $\text{RMSE} \approx 2.9 \times 10^{-3}$ ,  $\text{DA} \approx 72\%$ , full training speedup  $\approx 1.7\times$ , inference forward  $\approx 2.2\times$ ). For throughput oriented scenarios, QLSTM with batch 64 achieves maximum training throughput ( $2.23\times [2.20, 2.48]$ ) with reduced accuracy. For mixed workloads, QFWP with batch 32 provides a practical middle point ( $\text{RMSE} \approx 3.1 \times 10^{-3}$ ,  $\text{DA} \approx 70.2\%$ ) with about  $1.9\times$  speedup. These heuristics treat batching as a system level knob that jointly controls efficiency, gradient cost, and accuracy.

## Acknowledgements

The authors conducted all experiments on simulator backends that reflect state-vector dynamics rather than hardware noise, so timings represent relative efficiency. This work used PennyLane `lightning.qubit` (adjoint backend) on Windows 11 + WSL2 (Ubuntu 24.04.1 LTS) with an Intel Core Ultra 7 265K and 96 GB RAM.

The views expressed are those of the authors and do not represent Wells Fargo. This article is for informational purposes only and should not be construed as investment advice. Wells Fargo makes no express or implied warranties and disclaims any legal, tax, or accounting implications related to this article.

## 6. REFERENCES

- [1] Maria Schuld, Ilya Sinayskiy, and Francesco Petruccione, “An introduction to quantum machine learning,” *Contemporary Physics*, vol. 56, no. 2, pp. 172–185, 2015.
- [2] M. Schuld, “Quantum machine learning in feature hilbert spaces,” in *Advances in Quantum Machine Learning*, pp. 45–66. Springer, 2019.
- [3] Titouan Parcollet, Mohamed Morchid, Georges Linarès, and Renato De Mori, “Bidirectional quaternion long short-term memory recurrent neural networks for speech recognition,” in *ICASSP 2019-2019 IEEE International Conference on Acoustics, Speech and Signal Processing (ICASSP)*. IEEE, 2019, pp. 8519–8523.
- [4] Samuel Yen-Chi Chen, Shinjae Yoo, and Yao-Lung L Fang, “Quantum long short-term memory,” in *ICASSP 2022-2022 IEEE International Conference on Acoustics, Speech and Signal Processing (ICASSP)*. IEEE, 2022, pp. 8622–8626.
- [5] Samuel Yen-Chi Chen, “Learning to program variational quantum circuits with fast weights,” in *2024 International Joint Conference on Neural Networks (IJCNN)*. IEEE, 2024, pp. 1–9.
- [6] Chen-Yu Liu, Samuel Yen-Chi Chen, Kuan-Cheng Chen, Wei-Jia Huang, and Yen-Jui Chang, “Programming variational quantum circuits with quantum-train agent,” in *2025 International Conference on Quantum Communications, Networking, and Computing (QCNC)*. IEEE, 2025, pp. 544–548.
- [7] Mostafa Dehghani, Anurag Arnab, Lucas Beyer, Ashish Vaswani, and Yi Tay, “The efficiency misnomer,” *arXiv preprint arXiv:2110.12894*, 2021.
- [8] Samuel Yen-Chi Chen, Tzu-Chieh Wei, Chao Zhang, Haiwang Yu, and Shinjae Yoo, “Quantum convolutional neural networks for high energy physics data analysis,” *Physical Review Research*, vol. 4, no. 1, pp. 013231, 2022.
- [9] F. Hoch, G. Rodari, T. Giordani, P. Perret, N. Spagnolo, G. Carvacho, C. Pentangelo, S. Piacentini, A. Crespi, F. Ceccarelli, R. Osellame, and F. Sciarrino, “Variational approach to photonic quantum circuits via the parameter shift rule,” *arXiv preprint arXiv:2410.06966*, 2024.
- [10] Sepp Hochreiter and Jürgen Schmidhuber, “Long short-term memory,” *Neural computation*, vol. 9, no. 8, pp. 1735–1780, 1997.
- [11] Marco Cerezo, Andrew Arrasmith, Ryan Babbush, Simon C Benjamin, Suguru Endo, Keisuke Fujii, Jarrod R McClean, Kosuke Mitarai, Xiao Yuan, Lukasz Cincio, et al., “Variational quantum algorithms,” *Nature Reviews Physics*, vol. 3, no. 9, pp. 625–644, 2021.
- [12] Jürgen Schmidhuber, “Learning to control fast-weight memories: An alternative to dynamic recurrent networks,” *Neural Computation*, vol. 4, no. 1, pp. 131–139, 1992.
- [13] Jimmy Ba, Geoffrey E Hinton, Volodymyr Mnih, Joel Z Leibo, and Catalin Ionescu, “Using fast weights to attend to the recent past,” *Advances in neural information processing systems*, vol. 29, 2016.
- [14] Ville Bergholm, Josh Izaac, Maria Schuld, Christian Gogolin, Shahnawaz Ahmed, Vishnu Ajith, M Sohaib Alam, Guillermo Alonso-Linaje, B AkashNarayanan, Ali Asadi, et al., “PennyLane: Automatic differentiation of hybrid quantum-classical computations,” *arXiv preprint arXiv:1811.04968*, 2018.
- [15] Adam Paszke, Sam Gross, Francisco Massa, Adam Lerer, James Bradbury, Gregory Chanan, Trevor Killeen, Zeming Lin, Natalia Gimelshein, Luca Antiga, et al., “PyTorch: An imperative style, high-performance deep learning library,” *Advances in neural information processing systems*, vol. 32, 2019.
- [16] Frank Wilcoxon, “Individual comparisons by ranking methods,” *Biometrics bulletin*, vol. 1, no. 6, pp. 80–83, 1945.
- [17] Norman Cliff, “Dominance statistics: Ordinal analyses to answer ordinal questions.,” *Psychological bulletin*, vol. 114, no. 3, pp. 494, 1993.
- [18] Gene M Amdahl, “Validity of the single processor approach to achieving large scale computing capabilities,” in *Proceedings of the April 18-20, 1967, spring joint computer conference*, 1967, pp. 483–485.